Preprints.org

Article

Not peer-reviewed version

Uniform-Width Slotted Mm-Wave Antenna with Suppresed Sidelobe Level (SLL) And Enhanced Inter-Element Isolation

Jun Zhou , Heng Luo * , Haoran Jia , Yujie Zhang , Huanwei Duan , Huaizhong Chen , JIan Dong , Meng Wang , Chenwang Xiao

Posted Date: 5 March 2026

doi: 10.20944/preprints202603.0389.v1

Keywords: millimeter-wave antenna; sidelobe level; slotted patch; high-isolation; surface current distribution

Preprints.org is a free multidisciplinary platform providing preprint service that is dedicated to making early versions of research outputs permanently available and citable. Preprints posted at Preprints.org appear in Web of Science, Crossref, Google Scholar, Scilit, Europe PMC.

Copyright: This open access article is published under a Creative Commons CC BY 4.0 license, which permit the free download, distribution, and reuse, provided that the author and preprint are cited in any reuse.

Preprints.org (www.preprints.org) | NOT PEER-REVIEWED | Posted: 5 March 2026 doi:10.20944/preprints202603.0389.v1

Disclaimer/Publisher's Note: The statements, opinions, and data contained in all publications are solely those of the individual author(s) and contributor(s) and not of MDPI and/or the editor(s). MDPI and/or the editor(s) disclaim responsibility for any injury to people or property resulting from any ideas, methods, instructions, or products referred to in the content.

Article

Uniform-Width Slotted Mm-Wave Antenna with Suppresed Sidelobe Level (SLL) And Enhanced Inter-Element Isolation

Jun Zhou, Heng Luo *, Haoran Jia, Yujie Zhang, Huanwei Duan, Huaizhong Chen, Jian Dong, Meng Wang and Chenwang Xiao

School of Electronic Information, Central South University, Changsha 410004, P.R.China

* Correspondence: luohengcsu@csu.edu.cn

Abstract

High gain and low sidelobe level remain challenges for 5G millimeter-wave antenna systems. This paper presents a low-sidelobe, high-gain microstrip array antenna based on non-uniformly slotted identical-sized radiating patch, designed to simultaneously enhance gain and suppress sidelobe levels for 5G millimeter-wave (mmWave) communication systems. The key innovation lies in the use of an intermediate-deep, edge-shallow non-uniform slotting technique to precisely control the surface current distribution of the radiating elements. thereby achieving significant sidelobe level (SLL) suppression and antenna isolation enhancement without increasing the physical footprint of each element. The final design operates at a center frequency of 78.5 GHz, achieving a maximum gain of 15 dB and suppressing the first sidelobe below −20 dB, outperforming conventional linear arrays. Notably, the patch width is reduced to only 1 mm—compared to Chebyshev-distributed arrays—resulting in a compact array layout with over 40% unit width size reduction while simultaneously improving inter-element isolation by more than 18 dB. This current-distribution engineering approach offers a novel, structure-efficient pathway for designing high-performance, densely packed mmWave antenna arrays, circumventing the need for additional decoupling structures or enlarg the antenna spacing, simulation results show that the average isolation has increased by more than 5 dB from 76 GHz to 79 GHz. Finally, the same design method was used to design a 24GHz antenna, which was then fabricated and tested. The antenna achieved a sidelobe suppression of -17 dB.

Keywords: millimeter-wave antenna; sidelobe level; slotted patch; high-isolation; surface current distribution

1. Introduction

With the rapid development of intelligent vehicle technology and autonomous driving, automotive mmWave radar, as an important sensor for vehicle distance and speed measurement, is facing increasingly higher performance requirements [1–3]. Automotive mmWave radar mainly operates in the 24 GHz and 77 GHz frequency bands. The 24GHz radar has a lower cost and mature technology, with a moderate detection range, making it suitable for short- to medium-range applications such as blind spot detection. In contrast, the 77GHz radar is smaller in size, offers higher accuracy and resolution, and supports longer-range detection, making it more suitable for high-performance requirements such as autonomous driving; however, it comes with higher costs and technical barriers [4,5]. As an important component of mmWave radar, the antenna directly affects the radar's detection performance. The higher the antenna gain, the better the radar detection performance, which is also beneficial for improving the signal-to-noise ratio and enhancing radar reliability [6]. Lower SLL can reduce the radar's false alarm rate and improve anti-interference capability [7,8], with Chebyshev array synthesis and Taylor synthesis being common sidelobe suppression methods [9,10].

© 2026 by the author(s). Distributed under a Creative Commons CC BY license.

Preprints.org (www.preprints.org) | NOT PEER-REVIEWED | Posted: 5 March 2026 doi:10.20944/preprints202603.0389.v1

Faced with complex traffic environments, the gain of a single antenna is relatively small. To enable radar to measure longer distances, array technology holds significant research value [11,12]. Moreover, as radars move toward miniaturized and integrated designs, the antenna layout of the radar RF front end becomes increasingly important. Due to smaller spacing between antennas, strong coupling effects occur between array elements, leading to degraded radiation performance of the antenna system. Some researchers have adopted antenna decoupling structures to enhance isolation between array antennas [13,14].

This paper designs two 1×8 millimeter-wave radar array antennas with high gain, high isolation, and low sidelobes, which meet the application requirements for 24GHz and 77GHz automotive millimeter-wave radars, respectively. The array antenna uses a series-fed structure, achieving unequal amplitude distribution of current across the antennas by slotting elements of the same width, thereby suppressing sidelobes. Additionally, the antenna layout was analyzed, verifying that this antenna maintains good isolation when integrated into the radar RF front-end layout.Finally, a physical prototype of the 24GHz antenna array was fabricated and tested, and the test results validated the feasibility of the design scheme.

2. Design of Uniform-Width Slotted Millimeter-Wave Antenna

2.1. Antenna Array Configuration

Figure 1 shows a newly designed uniform-width slotted array antenna operating at 78.5 GHz. This antenna consists of three parts: the bottom metal ground plane, the middle dielectric substrate, and the top patch structure， The specific dimensions of the antenna patch are shown in Table 1.RO3003 was chosen as the dielectric substrate for the uniform-width slotted array antenna. It has an extremely low and stable loss factor of only 0.0013, which minimizes energy loss in the dielectric and ensures that more energy is radiated by the antenna. At the same time, RO3003 has a stable dielectric constant of 3. The upper radiation structure mainly consists of eight patch elements connected in series by microstrips, all with the same width. All patch elements except the first one are slotted. The last three antenna elements include an impedance matching structure, and a matching load structure is added at the end of the terminal elements.

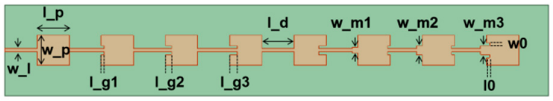

Figure 1. The layout of the 1×8 uniform-width slotted microstrip array.

Table 1. 77GHz Array Antenna Dimensions. (Units:mm).

Variable	**W_l**	**L_p**	**W_p**	**L_g1**	**L_g2**	**L_g3**
value	0.1	1.08	1	0.1	0.2	0.25
Variable	**l_d**	**w_m1**	**w_m2**	**w_m3**	**l0**	**w0**
value	0.97	0.2	0.3	0.3	0.1	0.1

Table 2. 24GHz Array Antenna Dimensions . (Units:mm).

Variable	**W_l**	**L_p**	**W_p**	**L_g1**	**L_g2**	**L_g3**
value	0.2	3.5	3.6	0.6	0.4	0.6
Variable	**l_d**	**w_m1**	**w_m2**	**w_m3**	**l0**	**w0**
value	3.5	0.2	0.2	0.5	0.5	0.3

© 2026 by the author(s). Distributed under a Creative Commons CC BY license.

Preprints.org (www.preprints.org) | NOT PEER-REVIEWED | Posted: 5 March 2026 doi:10.20944/preprints202603.0389.v1

2.2. Working Principle of Non-Uniform Slotted mmWave Antenna(78.5GHz)

In order to achieve high-gain, low-sidelobe performance for microstrip array antennas, the current intensity of different patch elements can be regulated. By reducing the weight of the edge elements, the energy sources that generate harmful coherent interference in non-main lobe directions are effectively weakened, thereby redistributing the radiated energy from the sidelobe regions to the main lobe direction and achieving SLL suppression. According to the principle of microstrip patch antennas, the patch antenna mainly radiates energy from the patch edges, with the current in the transmission line and the patch forming a sinusoidal distribution. To ensure maximum antenna radiation energy, each section of the transmission line and patch is initially designed to be half of the effective wavelength. The current intensity on both sides of the patch unit is equal but opposite in phas,and the current inside the patch unit has a sinusoidal distribution.By introducing slots on the patch, the length of the transmission line connecting the two patches is no longer half of the effective wavelength, and the connection between the microstrip line and the patch is not at the edge of the patch. As a result, the current intensity is not at its maximum, which affects the current intensity of the patch antenna.

The Figure 2 respectively show the relationship curves between the antenna SLL and the depths of gap1, gap2, and gap3. It is evident that the antenna SLL is significantly influenced by the depth variation of gap1, with smaller gap1 depths resulting in improved sidelobe suppression performance. For the left antenna, the SLL exhibits minimal variation when gap2 depth is set at 0.1mm or 0.2mm, but sidelobe suppression effectiveness declines at 0.3mm. In contrast, the right antenna demonstrates more consistent SLL across all lobes when gap2 depth is 0.2mm, accompanied by a reduced maximum SLL. The relationship between antenna SLL and gap3 depth variation follows a pattern analogous to that observed with gap2. When the depth of gap3 is 0.25mm, all SLL are relatively even, with a lower maximum SLL.It can be seen that the groove in the middle is slightly deeper, while the groove depth of the patch elements on both sides is slightly shallower, resulting in the best side lobe suppression for the antenna.

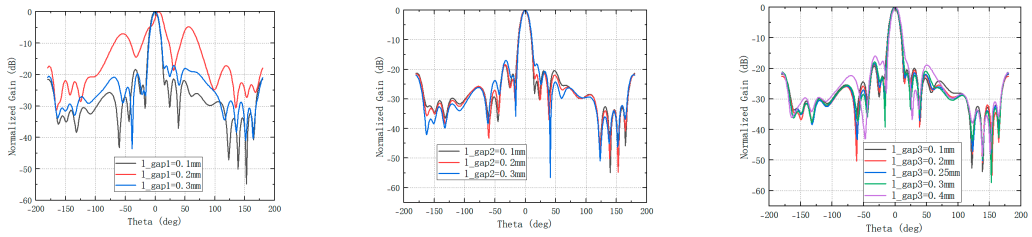

(**a**) (**b**) (**c**)

Figure 2. Relationship between antenna SLL and the depth of gap. (a) Relationship between antenna SLL and the depth of gap1; (b) Relationship between antenna SLL and the depth of gap2; (c) Relationship between antenna SLL and the depth of gap3.

Figure 3 shows the metal ground surface current density distributions of the uniform-width slotless antenna and the uniform-width slotted antenna. Observation shows that in the absence of slots on the antenna, the current intensity at locations corresponding to individual patches is nearly uniformly distributed.The introduction of slots into the antenna structure enables precise current distribution control, resulting in enhanced current density at the central unit positions while simultaneously suppressing current intensity at the peripheral unit locations. This engineered current modulation effectively concentrates the radiated energy within the main lobe region, thereby achieving significant SLL suppression.

© 2026 by the author(s). Distributed under a Creative Commons CC BY license.

Preprints.org (www.preprints.org) | NOT PEER-REVIEWED | Posted: 5 March 2026 doi:10.20944/preprints202603.0389.v1

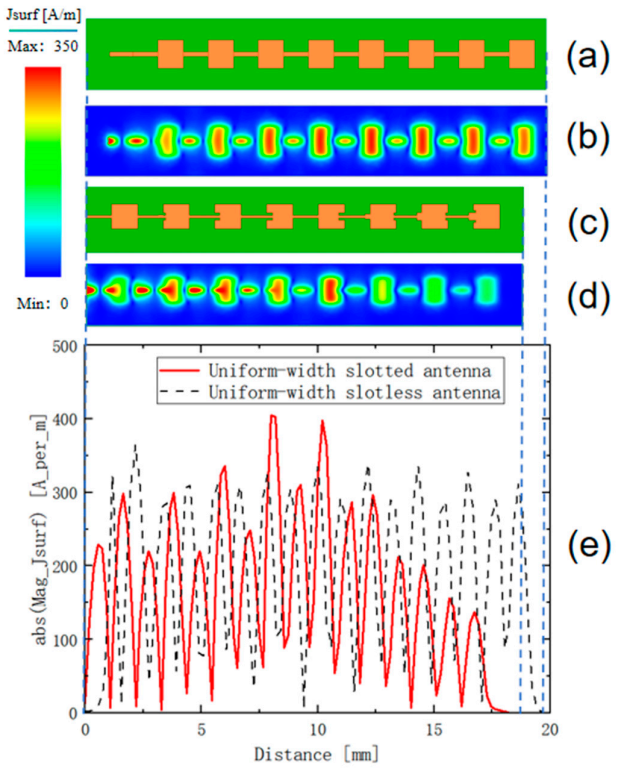

Figure 3. Surface Current Intensity Distribution of Antenna Metal Floor.

Figure 3 (e) shows the graph illustrating the spatial variation of current intensity along the distance from the feeding port.Each peak in the current distribution profile corresponds to a distinct microstrip line segment and patch unit. The current intensity exhibits a maximum value at the central two patch units and progressively diminishes toward the peripheral regions. Notably, the current density in patch units surpasses that of the microstrip line due to their wider physical dimensions and consequently lower characteristic impedance, which enables higher current carrying capacity.

To enhance the antenna's impedance matching performance, impedance matching structures are integrated into the last three patch units. This design mitigates the current intensity attenuation in the end patch caused by excessive mutual coupling among array elements. Furthermore, matching load structures are incorporated into the end patch units to absorb residual electromagnetic wave energy, thereby reducing cross-interference with adjacent electronic devices.

As shown in Figure 4 (a), after employing the impedance transformation structure, the uniform-width microstrip antenna achieves an S11 value of -40 dB around 78.5 GHz, indicating good impedance matching. The gain characteristics of the antenna over the frequency range of 76.5 GHz to 81 GHz are also presented, showing that the maximum gain occurs near 78.5 GHz, with a gain value exceeding 15 dB.At the same time, Figure 4 (b) shows that the uniform-width slotted antenna exhibits a clear suppression effect on sidelobe levels compared to conventional antenna. The first sidelobe level is reduced to below -20 dB, and all sidelobe levels are maintained below -18 dB.

© 2026 by the author(s). Distributed under a Creative Commons CC BY license.

Preprints.org (www.preprints.org) | NOT PEER-REVIEWED | Posted: 5 March 2026 doi:10.20944/preprints202603.0389.v1

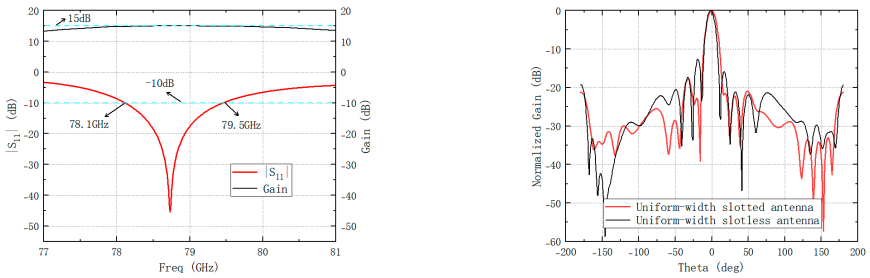

(**a**) (**b**)

Figure 4. Performance of uniform-width slotted microstrip array antenna.(a) Antenna S11 Parameters and Gain;(b) Antenna side lobe level.

3. Analysis of the Layout of Uniform-Width Slotted Microstrip Array Antenna(78.5GHz)

A single-antenna design exhibits inherently limited gain capability and lacks the flexibility to adapt beam patterns to diverse radar detection requirements, thereby failing to satisfy the multi-target detection demands of vehicle-mounted mmWave radar systems. The antenna layout configuration plays a pivotal role in radar performance optimization.As shown in Figure 5, this study conducts layout simulation analysis of both the proposed non-uniform slotted array antenna and the conventional Chebyshev low-sidelobe array antenna based on the antenna architecture of the Texas Instruments AWR2944 millimeter-wave radar chip. The AWR2944 employs a 4×4 MIMO (Multiple-Input Multiple-Output) RF front-end configuration, comprising four transmit (TX) and four receive (RX) antenna elements. To ensure phase coherence of signals arriving at each antenna, the transmission lines connecting the chip to the antenna array are meticulously designed with equal electrical lengths. Furthermore, the spatial arrangement of transmit antennas is optimized to achieve two critical objectives: (1) maintaining perfect synchronization between TX and RX antenna pairs, and (2) avoiding both excessive element spacing that leads to area inefficiency and virtual array duplication that degrades spatial resolution. Specifically, the intervals between TX1-TX3 and TX1-TX4 are set to four half-wavelengths ($4\lambda/2$), while TX2 is strategically positioned to facilitate elevation angle estimation through phase difference measurement.

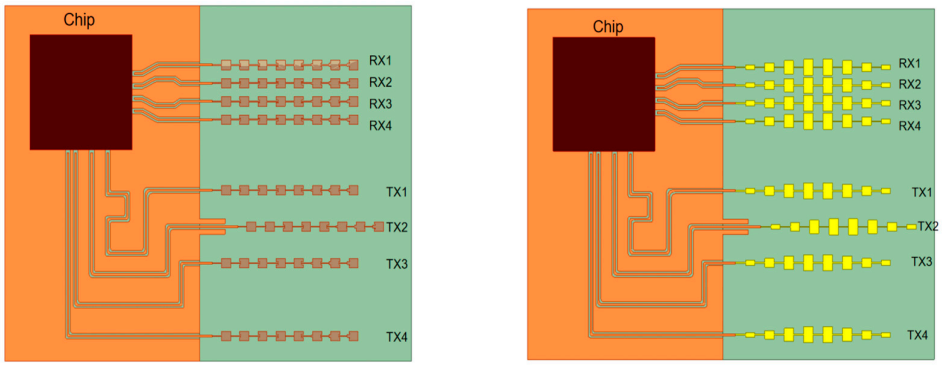

(**a**) (**b**)

Figure 5. 4-transmit 4-receive array antenna layout.(a)Uniform-width slotted array layout;(b)Chebyshev array layout.

In order to ensure effective signal transmission between the chip and the antenna, impedance matching between the transmission line connected to the antenna and the RF circuit is very important. Figure 6（a） shows the relationship between transmission line width and reflection coefficient. As

© 2026 by the author(s). Distributed under a Creative Commons CC BY license.

Preprints.org (www.preprints.org) | NOT PEER-REVIEWED | Posted: 5 March 2026 doi:10.20944/preprints202603.0389.v1

the transmission line width increases, impedance matching improves, but at the same time, the sidelobe suppression of the antenna becomes worse. Therefore, a transmission line width of 0.4mm is chosen to ensure good impedance matching while maximizing the suppression of the antenna's SLL. Additionally,Figure 6（b） shows that the SLL on the left side of the antenna are noticeably higher than those on the right side, which is caused by some energy radiating from the transmission line on the left side of the antenna.

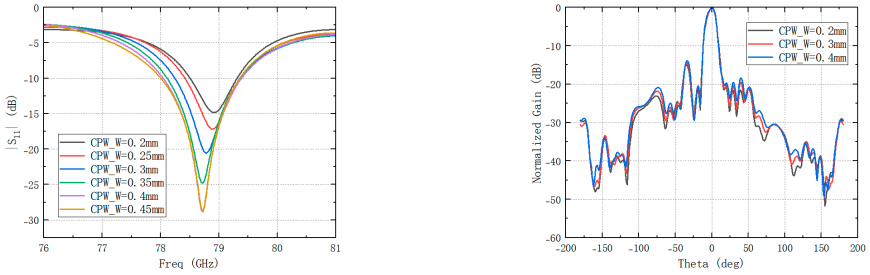

(**a**) (**b**)

Figure 6. Impact of Transmission Line Width on Antenna Performance.（a）The impact of transmission line width on the antenna reflection coefficient;（b）The impact of Transmission Line Width on Antenna SLL.

Figure 7 shows the overall antenna gain when RX1 is excited alone versus when both RX1 and RX2 are excited simultaneously. It can be seen that when both ports are excited at the same time, the antenna gain increases, and the antenna beamwidth becomes narrower, resulting in better antenna directivity.

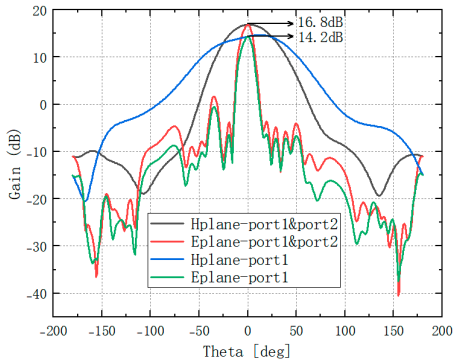

Figure 7. Single-port excitation and dual-port excitation antenna gain.

Figure 8 shows the curves of the S21 parameters of the two antennas versus frequency. It can be seen that the slotted low-sidelobe array antenna designed in this paper has an S21 parameter that is on average more than 5 dB lower in the 76-79 GHz range compared to the traditional Chebyshev low-sidelobe array antenna, and the isolation between antennas is better.This is because the maximum unit size of the array patch designed in this paper is only 1 millimeter, which is approximately 40% smaller than the maximum width of 1.7 millimeters of the Chebyshev array patch.With the spacing between the two antennas kept equal, the patches in the Chebyshev array are closer together, resulting in stronger coupling effects between adjacent antennas.

© 2026 by the author(s). Distributed under a Creative Commons CC BY license.

Preprints.org (www.preprints.org) | NOT PEER-REVIEWED | Posted: 5 March 2026 doi:10.20944/preprints202603.0389.v1

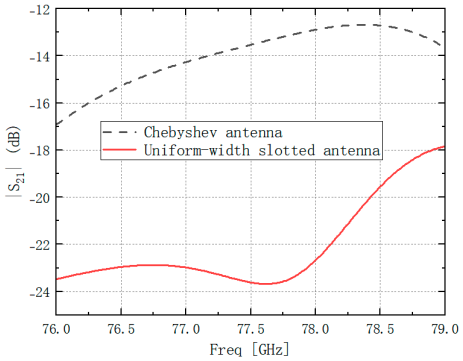

Figure 8. Comparison of isolation between Uniform-width slotted antenna and Chebyshev array antenna.

4. Implementation and Measurement

Due to the high cost of manufacturing 77GHz array antennas and the stringent requirements of the testing equipment, in order to verify the feasibility of the above design scheme, we conducted a fabrication test on a 24GHz array antenna. The finished antenna array is shown in Figure 9(a), and the comparison results between simulation and actual measurements are shown in Figure 9(b) and Figure 9(c).From the simulation and test results, It can be seen that this antenna mainly operates in the 24 GHz frequency band, with a return loss coefficient below -15dB at 24 GHz.. With the design of an equal-width non-uniform slotted structure, the antenna exhibits good sidelobe suppression, with overall sidelobes suppressed below -17 dB. The simulation and test results show a high degree of correlation, but there are some fluctuations. This is because millimeter-wave antennas are small in size and may have certain dimensional errors during fabrication, and the antenna is relatively thin, making it prone to bending and other unstable factors that cause errors.

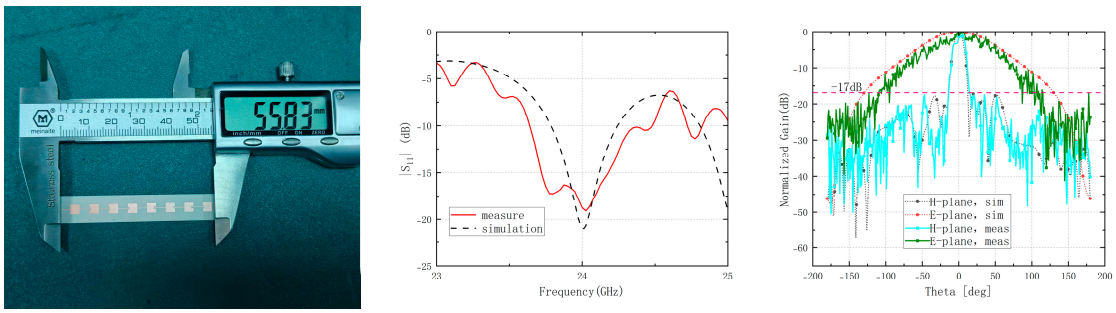

(**a**) (**b**) (**c**)

Figure 9. Antenna physical model and test results.(a)Antenna physical model;(b)|S11|;(c)Normalized Gain.

5. Conclusions

This paper proposes a novel design method for high-gain, low-sidelobe microstrip uniform-width array antennas.The antenna adopts a non-uniform slot structure, with deep slots in the middle patch elements and shallow slots in the side elements, effectively regulating the antenna current distribution, thereby better focusing energy on the main beam and achieving efficient suppression of sidelobe levels. Additionally, for the last three patch elements, an impedance matching structure is designed to better direct energy into the terminal patch element. Based on this method, an antenna was designed that achieves good impedance matching in the 78.1 GHz to 79.5 GHz frequency band, with a gain of 15 dB and overall sidelobe levels suppressed below -18 dB. This paper also conducts a layout analysis of the designed antenna. Compared with a single antenna, reasonably increasing the

© 2026 by the author(s). Distributed under a Creative Commons CC BY license.

Preprints.org (www.preprints.org) | NOT PEER-REVIEWED | Posted: 5 March 2026 doi:10.20944/preprints202603.0389.v1

number of antennas and adopting a proper layout method can further enhance antenna gain. Due to the unique uniform-width structure of the antenna patches, compared with traditional Chebyshev low-sidelobe array antennas, the maximum width is smaller, allowing for larger spacing between antennas and improving inter-antenna isolation. Simulation results show that the uniform-width array antenna with added slots achieves an average improvement of about 5dB in isolation compared with the Chebyshev array antenna from 76GHz to 79GHz.

Finally, an array antenna operating at 24 GHz was fabricated using the same equal-width grooved design method. The antenna's sidelobe levels were suppressed below -17 dB, verifying the effectiveness of the antenna design method.

Author Contributions: Simulation optimization, validation, formal analysis, writing—original draft, and visualization were performed by Jun Zhou. Resource coordination, writing—review and editing, supervision, and funding acquisition were carried out by Heng Luo. Problem-solving assistance was provided by Haoran Jia, Yujie Zhang, Huaizhong Chen, Huanwei Duan, Jian Dong, Meng Wang, and Chengwang Xiao. All authors have read and agreed to the published version of the manuscript.

Funding: This work was funded in part by the National Natural Science Foundation of China under Grant 61801521 and Grant 61971450, and in part by the Natural Science Foundation of Hunan Province under Grant 2018JJ2533, Grant 2022JJ30052, and Grant 2023JJ40775.

Data Availability Statement: The datasets generated during and/or analysedduring the current study are available from thecorresponding author on reasonable request.

Acknowledgments: In the course of this research, the authors utilized software tools including Ansys HFSS for electromagnetic modeling and optimization analysis, and Origin for data visualization and graphical presentation of results. The capabilities of these software packages were instrumental in facilitating the study and effectively communicating the findings, for which the authors express their gratitude.

Conflicts of Interest: The authors declare no conflicts of interest.

Abbreviations

The following abbreviations are used in this manuscript:

SLL	Suppresed Sidelobe Level
mmWave	millimeter-wave

References

1. Y. Cai, J. Bai, H. L. Shen, L. Huang, B. Rao, and H. Wang, “Development of Low-Cost Single-Chip Automotive 4D Millimeter-Wave Radar,” (J), Sensors (Basel), vol. 25, no. 15, pp. 4640–4640, Jul. 26 2025., doi: 10.3390/s25154640
2. Sakurai R, Hirokawa J, Tomura T .Waveguide 3×2-slot subarray antenna for millimeter-wave car radar[J].IEICE Communications Express,2025,14(4):155-158.DOI:. 10.23919/comex.2024XBL0211
3. Tan B, Ma Z, Zhu X, et al.Tracking of Multiple Static and Dynamic Targets for 4D Automotive Millimeter-Wave Radar Point Cloud in Urban Environments[J].Remote Sensing,2023,15(11):2923-.DOI:. 10.3390/rs15112923
4. D. Bu, S.-W. Qu; BuD, “QuS. Magneto-electric dipole antenna array for 77 GHz automotive radar,” (J), IET Microw. Antennas Propag., vol. 18, no. 2, pp. 96–105, 2023., doi: 10.1049/mia2.12445
5. Q. Chen, S. Yan, X. Guo, W. Wang, Z. Huang, L. Yang, et al., “A low sidelobe 77 GHz centre-fed microstrip patch array antenna,” (J), IET Microw. Antennas Propag., vol. 17, no. 11, pp. 887–896, 2023., doi: 10.1049/mia2.12408
6. S. A. Yong and K. Boumseock, “High Gain Diagonally-Probe-Fed Multi-Layered Dielectric Resonator Antenna Array for 77 GHz Automotive Radar Applications,” (J), J. Infrared Millim. Terahertz Waves, vol. 45, no. 3-4, pp. 349–369, 2024., doi: 10.1007/s10762-024-00978-x

© 2026 by the author(s). Distributed under a Creative Commons CC BY license.

Preprints.org (www.preprints.org) | NOT PEER-REVIEWED | Posted: 5 March 2026 doi:10.20944/preprints202603.0389.v1

7. J. Zhou, Q. Wang, Y. Yang, Y. Li, K. Kang, and H. Tang, "A 77 GHz Millimeter-Wave Comb Antenna With Suppressed Side-Lobe," (J), Microw. Opt. Technol. Lett., vol. 67, no. 4, pp. e70185–e70185, 2025., doi: 10.1002/mop.70185
8. J. Zhu and J. Liu, "Design of Microstrip Antenna Integrating 24 GHz and 77 GHz Compact High-Gain Arrays," (J), Sensors (Basel), vol. 25, no. 2, pp. 481–481, Jan. 16 2025., doi: 10.3390/s25020481
9. L. Li, Y. Dong, X. Cai, and J. Tian, "An Antenna Array with Wide Flat-Top Beam and Low Sidelobes for Aerial Target Detection," (J), Sensors (Basel), vol. 25, no. 19, pp. 5991–5991, Sep. 28 2025., doi: 10.3390/s25195991
10. J. Jung, Y. Park, and J. Ryu, "JungJ, ParkY, RyuJ. Enhanced Phase Coherence in Series-Fed Patch Array Antenna: A Design Method for Uniform Element Spacing With Low Sidelobe Levels," (J), Microw. Opt. Technol. Lett., vol. 66, no. 12, pp. e70066–e70066, 2024., doi: 10.1002/mop.70066
11. S. Rajpoot, S. G. Baghel, and M. Swati, Design of a compact, wideband, Diagonal Square Fractal MIMO antenna for vehicular communication [J] AEUE - International Journal of Electronics and Communications, 2025, pp. 202156023–156023, . 10.1016/j.aeue.2025.156023
12. J. Pillai, J. Prajapati, and D. M. Upadhayay, "Wide Half Power Beamwidth MIMO Antenna for Vehicular Radar System," (J), Int. J. Appl. Electromagn. Mech., vol. 77, no. 4, pp. 276–290, 2025., doi:
13. KURIYAMA A, NAGAISHI H, KURODA H, et al.Horn and Lens Antenna with Low Height and Low Antenna Coupling for Compact Automotive 77-GHz Long-Range Radar:Special Section on Microwave and Millimeter-Wave Technologies[J].IEICE Transactions on Electronics,2020,E103.C(10):426-433.DOI:. 10.1587/transele.2020MMP0002
14. M. Bakhshi, V. Faramarzi, H. S. Ayatollahi, et al., Enhanced 2-port MIMO antenna with composite two-step metasurface for 77 GHz Vehicle-to-Everything applications [J] AEUE - International Journal of Electronics and Communications, 2024, pp. 184155404–155404, . 10.1016/j.aeue.2024.155404

Disclaimer/Publisher's Note: The statements, opinions and data contained in all publications are solely those of the individual author(s) and contributor(s) and not of MDPI and/or the editor(s). MDPI and/or the editor(s) disclaim responsibility for any injury to people or property resulting from any ideas, methods, instructions or products referred to in the content.

© 2026 by the author(s). Distributed under a Creative Commons CC BY license.